MOLECULAR AND CELLULAR BIOLOGY, Sept. 2006, p. 6870–6879 Vol. 26, No. 18
0270-7306/06/$08.00+0 doi:10.1128/MCB.00314-06

Pleiotropic Phenotype of a Genomic Knock-In of an RGS-Insensitive G184S Gnai2 Allele

Xinyan Huang,[1] Ying Fu,[1] Raelene A. Charbeneau,[1] Thomas L. Saunders,[2] Douglas K. Taylor,[3] Kurt D. Hankenson,[3,4] Mark W. Russell,[5] Louis G. D'Alecy,[6,7] and Richard R. Neubig[1]*

Department of Pharmacology,[1] Department of Internal Medicine, Transgenic Animal Model Core,[2] Unit for Laboratory Animal Medicine,[3] Departments of Biomedical Engineering, Cell and Developmental Biology, and Orthopaedic Surgery,[4] Department of Pediatrics and Communicable Diseases,[5] and Departments of Molecular and Integrative Physiology and Vascular Surgery,[6] University of Michigan, Ann Arbor, Michigan, and Department of Surgery, William Beaumont Hospital, Royal Oak, Michigan[7]

Received 20 February 2006/Returned for modification 12 June 2006/Accepted 23 June 2006

Signal transduction via guanine nucleotide binding proteins (G proteins) is involved in cardiovascular, neural, endocrine, and immune cell function. Regulators of G protein signaling (RGS proteins) speed the turn-off of G protein signals and inhibit signal transduction, but the in vivo roles of RGS proteins remain poorly defined. To overcome the redundancy of RGS functions and reveal the total contribution of RGS regulation at the $G\alpha_{i2}$ subunit, we prepared a genomic knock-in of the RGS-insensitive G184S Gnai2 allele. The $G\alpha_{i2}^{G184S}$ knock-in mice show a dramatic and complex phenotype affecting multiple organ systems (heart, myeloid, skeletal, and central nervous system). Both homozygotes and heterozygotes demonstrate reduced viability and decreased body weight. Other phenotypes include shortened long bones, a markedly enlarged spleen, elevated neutrophil counts, an enlarged heart, and behavioral hyperactivity. Heterozygous $G\alpha_{i2}^{+/G184S}$ mice show some but not all of these abnormalities. Thus, loss of RGS actions at $G\alpha_{i2}$ produces a dramatic and pleiotropic phenotype which is more evident than the phenotype seen for individual RGS protein knockouts.

Cell-cell communication is fundamental to the maintenance of homeostasis. The G protein-coupled receptor superfamily is arguably the most abundant and diverse protein family in cellular signaling and is tightly regulated. A novel family of >20 proteins termed regulators of G protein signaling, or RGS proteins, both tonically inhibit G protein function and also serve as signal control points (2, 22, 34, 39, 69). RGS-mediated inhibition of G protein signaling occurs through direct binding of the RGS protein to the Gα subunit, with subsequent GTPase-accelerating protein (GAP) actions to rapidly deactivate Gα (2). Deactivation may be accelerated up to 1,000-fold and shuts down both Gα and Gβγ signals (42, 48). RGS proteins may also competitively inhibit Gα binding to effectors such as phospholipase C (32). Most of the currently known RGS proteins interact with either Gi or Gq family G proteins and influence cyclic AMP (cAMP), Ca^{2+}, mitogen-activated protein kinase, and ion channel signaling. There is strong evidence implicating them in the subsecond kinetics of G_i- and G_o-mediated ion channel activation and deactivation in the heart (10, 21, 36) and neurons (36). In addition, the conserved RGS domain has been found to serve as a multifunctional protein adapter which can recruit many effectors or regulators to the vicinity of activated G proteins (31, 53, 62). Notable examples include p115rhoGEF (30, 40) and GRK2 (44). There is also emerging interest in RGS proteins as drug targets (9, 20, 53, 72).

However, the physiological functions of RGS proteins remain poorly defined. A number of RGS knockouts have been reported (for example, RGS1, -2, -4, and -9). The RGS9-1 knockout shows prolonged visual potentials (7), and RGS9-2 disruption results in markedly enhanced responses to drugs of abuse, such as cocaine, amphetamines, and opiates (56, 71). A human disorder, bradyopsia, with reduced visual acuity for rapidly moving objects, has been identified with loss of RGS9-1 or its membrane anchor (54). The RGS2 knockout was initially reported to have only subtle behavioral and immunologic phenotypes but was subsequently found to be markedly hypertensive (33). RGS4 (26) and RGS1 (28, 46) knockouts have subtle effects on sensorimotor functioning and lymphocyte trafficking, respectively. One difficulty in unraveling the function of RGS proteins has been the complex interactions of the many subtypes of both G proteins and RGS proteins. This redundancy of RGS function limits an understanding of the RGS role in vivo, since standard antisense or knockout strategies targeting a single RGS gene will underestimate the overall role of RGS proteins.

To determine the full contribution of RGS proteins as a group to biological responses mediated by a particular G protein (e.g., G_o and G_i), we took advantage of a G alpha-subunit point mutation first found in the yeast *Saccharomyces cerevisiae* (19) that prevents RGS binding to the Gα subunit and GAP activity. The analogous mutation (Gly^{184} to Ser) in mammalian $G\alpha_o$ and $G\alpha_{i1}$ prevented the GAP activity of RGS4 and RGS7 and blocked RGS4 binding to aluminum fluoride-activated Gα subunits (41). These mutations do not affect other functions of the Gα subunit, such as the intrinsic GTPase activity of the G protein or its coupling to βγ subunits, receptors, GRK, or effectors (adenylyl cyclase [AC]) (18, 25). Thus, the only known effect of the G184S mutation in $G\alpha_o$ and $G\alpha_i$ is to prevent RGS action on Gα. Several publications using overexpression of these RGS-insensitive Gα subunits revealed profound slow-

* Corresponding author. Mailing address: Department of Pharmacology, University of Michigan, 1301 MSRB III, Ann Arbor, MI 48109. Phone: (734) 763-3650. Fax: (734) 763-4450. E-mail: rneubig@umich.edu.

ing of channel response kinetics and/or increased potency of agonist responses in neurons (8, 11–13, 37).

Signaling by the Gi family of "inhibitory" G proteins is complex. While they inhibit adenylyl cyclase, G_i proteins can also activate or inhibit many other effectors through either the GTP-bound $G\alpha_i$ or the $\beta\gamma$ subunit released upon activation. Indeed, $\beta\gamma$ is commonly implicated in G_i signaling and so, unlike $G\alpha_s$ and $G\alpha_q$, overexpression of mutant $G\alpha_i$ proteins will not fully mimic the response. Specifically, $G\beta\gamma$ inhibits N-type Ca^{2+} channels and activates G protein-coupled inwardly rectifying K^+ (GIRK) channels, phospholipase C β_2, and phosphatidyl inositol 3-kinase γ isoforms (17, 51). In addition, $\beta\gamma$ released from G_i can activate ERK through complex and cell-type-specific mechanisms (55). Along with Gq, the Gi family of G proteins is most strongly regulated by RGS proteins, and expression of $G\alpha_{i2}$ is ubiquitous. Surprisingly, knockouts are viable (58), perhaps due to redundancy with related $G\alpha$ subunits ($G\alpha_{i1}$ and $G\alpha_{i3}$).

In the present study, we prepared a genomic knock-in of the RGS-insensitive $G\alpha_{i2}^{G184S}$ allele to assess the role of RGS proteins in the function of $G\alpha_{i2}$ and to probe the physiological functions of $G\alpha_{i2}$. A knock-in was used instead of a transgenic model to maintain the normal distribution and level of $G\alpha_{i2}$ protein expression. Since the mutant $G\alpha_{i2}^{G184S}$ protein can't be turned off by RGS proteins, we expected that in any tissue with functional RGS activity at $G\alpha_{i2}$, we would see enhanced, but receptor-dependent, G_{i2} activity. Indeed, the $G\alpha_{i2}^{G184S/G184S}$ homozygous mutant mice showed enhanced signaling and a dramatic and pleiotropic physiological phenotype, including reduced viability, low birth weight, growth retardation, cardiac hypertrophy, enlarged spleen, elevated neutrophil and monocyte counts, and behavioral hyperactivity, while heterozygotes showed some elements of the phenotype.

MATERIALS AND METHODS

Materials. Pertussis toxin (PTX) was from List Biological Laboratories (Campbell, CA), forskolin was from Calbiochem (LaJolla, CA), and isobutyl-1-methylxanthine, ATP, cAMP, and lysophosphatidic acid (LPA) were from Sigma (St. Louis, MO).

Generation of $G\alpha_{i2}^{G184S/G184S}$ mice. All protocols and procedures were approved by the University Committee on Use and Care of Animals, and animal care was overseen by the Unit for Laboratory Animal Medicine (University of Michigan). The production of the $G\alpha_{i2}^{G184S/G184S}$ mice has been described in detail in the supporting online material of Fu et al. (24). Briefly, the targeting construct pTKLNL/$G\alpha_{i2}^{G184S}$ harbors a 5′ sequence encoding thymidine kinase followed by a 13.8-kb $G\alpha_{i2}$ genomic sequence that is divided into two regions of $G\alpha_{i2}$ homology (6.7 and 7.1 kb in size) surrounding a loxP-flanked *neo* cassette. Homologous recombination between the targeting construct and the targeted locus leads to a modified $G\alpha_{i2}$ gene (Fig. 1A) that contains the positively selectable gene *neo* and the G184S missense mutation located in exon 5, encoded by a GGC→TCG change, which also adds a diagnostic PvuI restriction site. Targeted CJ7 embryonic stem (ES) cells derived from 129S1/SvImJ (64) were microinjected into C57BL/6NCrl × (C57BL/6J × DBA/2J)F_1 mouse blastocysts to generate ES cell-mouse chimeras. Mutant mice ($G\alpha_{i2}^{+/G184Sneo}$) were generated by crossing male chimeras with C57BL/6J female mice. Germ line transmission of the G184Sneo allele was identified by Southern blot detection of a 12-kb SacI band (Fig. 1B, middle lane) due to insertion of the *neo* cassette, while the wild-type (wt) allele shows a 10-kb band (Fig. 1B, left lane). Female heterozygous mice ($G\alpha_{i2}^{+/G184Sneo}$) were crossed with C57BL/6J-TgN(Zp3-cre)93Knw mice (Jax; stock no. 003651) (43) to delete the *neo* cassette. After one more cross with C57BL/6J mice, the offspring had lost the *neo* cassette, as shown by Southern blotting (Fig. 1B, right lane) and by PCR with primers c and d flanking the remaining *loxP* site (Fig. 1A): c, 5′-CAC ACT TCA CCT TCA AGG AC-3′; d, 5′-CTG ATG CCT AGG TGA CAG AC-3′. The wild-type allele (no loxP) produces a band of 181 bp while the inserted loxP leads to a band at 361 bp (Fig. 1C), and the intact loxP-*neo*-loxP allele is not detected due to the large size of the product. To ensure that the G184S mutation was carried along with the *neo* or loxP markers, mouse tail genomic DNA was screened by PCR amplification followed by PvuI digestion of the product. The forward primer a was 5′-GGA GCGCATTGCACAGAG-3′, and the reverse primer b was 5′-GCAGCTATG GCCCTTAAC-3′ (Fig. 1A). The appearance of the 140-bp product after PvuI digestion indicates the presence of the G184S mutation (Fig. 1D).

Animals. Heterozygous ($G\alpha_{i2}^{+/G184S}$) mice used in this study had been backcrossed for 4 to 7 generations onto the C57BL/6J strain. The homozygous ($G\alpha_{i2}^{G184S/G184S}$) mice were generated by heterozygote crosses. Animals were maintained on a 12-h light/12-h dark schedule and fed standard laboratory chow and water ad libitum. Age- and gender-matched littermates were used for all experiments. All mice used in this study were between 13 and 22 weeks of age, and the number of mice for each study is indicated in the figure legends.

Tissue and blood analyses. Mice were sacrificed by CO_2 inhalation in the morning at 20 to 22 weeks of age to obtain either blood or tissue samples. Blood was collected from the orbital sinus into EDTA dipotassium salt-coated microtubes (Sarstedt Aktlengesellschaft & Co., Germany). Tissues were removed, weighed, frozen in liquid nitrogen, and stored at −70°C until processed for analysis. The femur and tibia were dissected, and the length and width were measured using calipers. A complete blood count with differential count was performed by the Animal Diagnostic Laboratory Unit for Laboratory Animal Medicine of the University of Michigan.

G protein expression. Tissue was taken rapidly from animals killed by CO_2 inhalation. Heart, liver, and brain tissues were snap-frozen using liquid nitrogen and stored at −80°C. Extracts of tissues from control or $G\alpha_{i2}^{G184S/G184S}$ mice were prepared as described by Koch (38), and an equal amount of protein (40 to 100 μg) from paired controls was fractionated by sodium dodecyl sulfate-polyacrylamide gel electrophoresis and immunoblotted with a $G\alpha_{i2}$-specific antiserum (J883) (49, 50) kindly provided by Susanne Mumby (University of Texas Southwestern Medical Center). The blots were then stripped and reprobed with an anti-G-protein β-subunit antibody (sc-378; Santa Cruz Biotechnology) as a control for protein loading.

MEF culture. Mouse embryonic fibroblast (MEF) lines were isolated by trypsinization of separate embryos at embryonic day 13.5 as described elsewhere (66). Homogenous cell suspensions were maintained and expanded at 37°C in high-glucose Dulbecco's modified Eagle's medium (DMEM; Gibco BRL) supplemented with 10% (vol/vol) bovine serum (Gibco BRL). A 3T3 protocol (66) was performed to establish cell lines; that is, every 3 days, cells were trypsinized and counted, and 3×10^5 cells were plated per 60-mm dish. Three each of the $G\alpha_{i2}$ wild-type, heterozygous (+/G184S), and homozygous (G184S/G184S) cell lines were established.

Whole-cell cAMP production. cAMP production in MEF cells (see "MEF culture," above) was determined in 24-well plates as described by Wade et al. (68), and inhibition by LPA was assessed. Briefly, MEF cells (passage 5 and below) were plated at 20,000 cells per well and incubated with 1 μCi/well [^{3}H]adenine for 18 to 20 h. Cells were washed once with DMEM, and cAMP accumulation was initiated by adding DMEM containing 1 mM isobutyl-1-methylxanthine and 10 μM forskolin with the indicated concentrations of LPA. After 30 min at 37°C, acid-soluble nucleotides were collected and separated on Dowex and alumina columns as described previously (60).

ERK and Akt phosphorylation. MEF cells (passage 30 or above; see "MEF culture," above) were seeded in six-well culture plates and incubated at 37°C in a humidified incubator containing 5% CO_2 in air until ~80% confluent. Cells were then incubated with DMEM supplemented with 0.5% fetal bovine serum overnight to minimize basal Akt and ERK phosphorylation. For PTX treatment, 100 ng/ml PTX was included during the overnight serum starvation. After activation with the indicated concentrations of LPA for 7.5 min, medium was removed, and cells were washed with cold phosphate-buffered saline before addition of phospho-homogenization buffer (20 mM Tris-HCl [pH 7.5], 150 mM NaCl, 1 mM Na_2EDTA, 1% Triton X-100, 2.5 mM sodium pyrophosphate, 1 mM β-glycerophosphate, 1 mM Na_3VO_4, and 1 μg/ml leupeptin). Homogenates were scraped into 1.5-ml tubes and centrifuged (13,793 × *g*, 20 min, 4°C), and supernatants were retained for phosphoprotein analysis. Samples were subjected to sodium dodecyl sulfate-polyacrylamide gel electrophoresis on 12% gels and transferred to Immobilon-P, probed with monoclonal antibodies against phospho-ERK1/2 (Thr202/Tyr204; Cell Signaling Technology, Beverly, MA) and phospho-Akt (Ser473; Cell Signaling Technology), and visualized with chemiluminescence. Bands were quantitated on a Kodak Image Station 440CF and analyzed with the Kodak 1D Image Analysis software. The blot was subsequently stripped and reprobed with ERK- and Akt-specific antibodies (Cell Signaling Technology) to assess total kinase expression. Ratios of phosphorylated versus

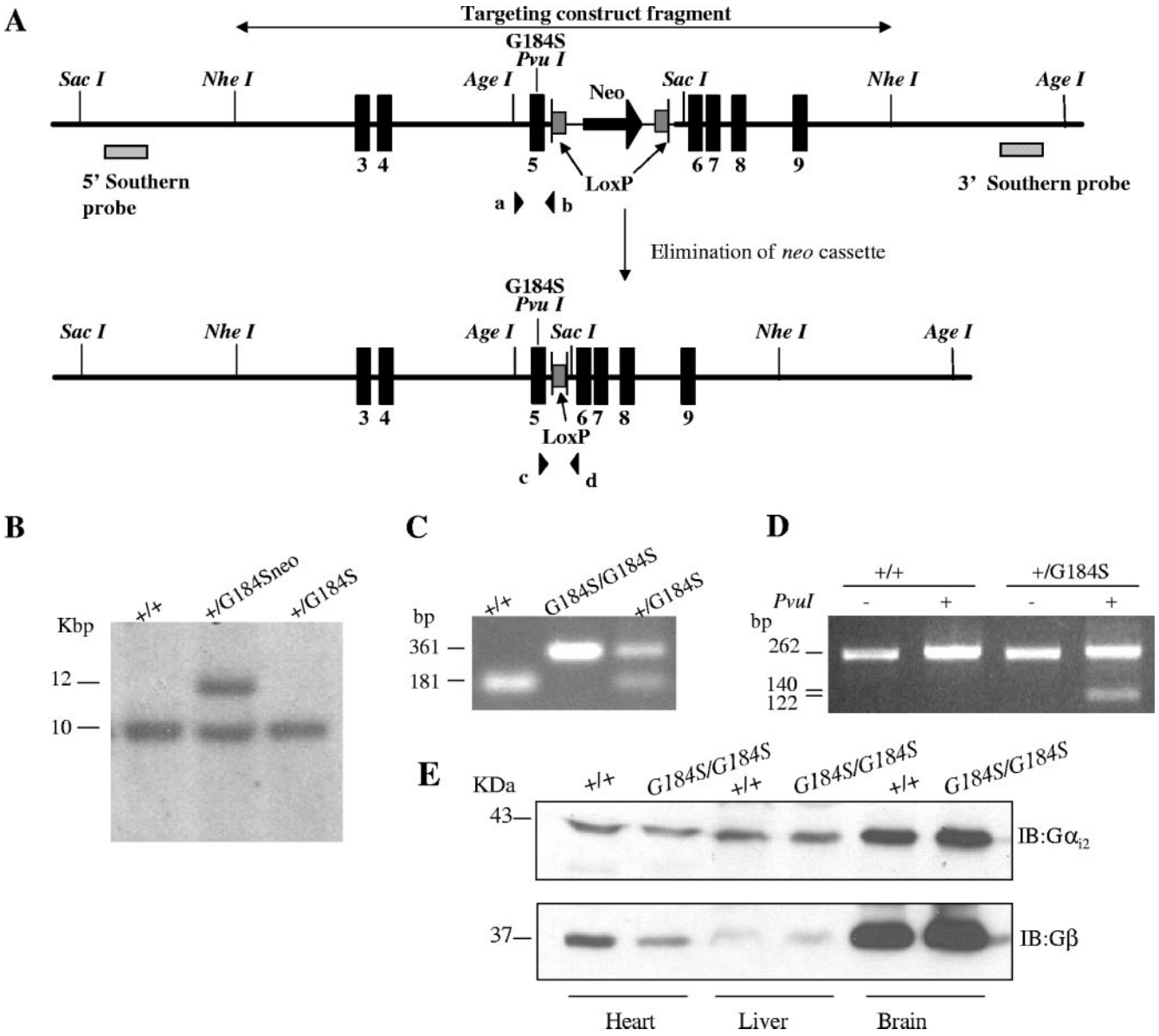

FIG. 1. Gene targeting strategy and biochemical and genetic confirmation. (A) Targeted $G\alpha_{i2}^{G184Sneo}$ genomic fragment. Top: Mouse $G\alpha_{i2}^{G184Sneo}$ genomic fragment after homologous recombination. Homologous recombination incorporates the G-to-S mutation into the genomic DNA along with a diagnostic PvuI restriction site and a *neo* resistance gene flanked by loxP sites inserted in intron 5, 116 bp from the point mutation. Bottom: Scheme for removal of the *neo* cassette. Female heterozygous mice ($G\alpha_{i2}^{+/G184Sneo}$) were mated with male C57BL/6J-TgN(Zp3-cre)93Knw mice. After two generations, the *neo* cassette is eliminated. (B) Homologous recombination and *neo* removal demonstrated by Southern blot analysis in ES cells. In SacI digests, a 5′ Southern blotting probe recognizes two bands for the targeted heterozygous (+/G184Sneo) cells (middle lane) by the appearance of a 12-kb G184Sneo band, whereas only a 10-kb band is present in wild-type (+/+) cells (left lane) and cells transfected with a *cre* recombinase plasmid (right lane). Similar results were seen in the offspring (+/G184S) that had lost the *neo* cassette. (C) PCR screening confirms the in vivo loss of the *neo* cassette with primers (c and d) flanking the two loxP sites. For both heterozygous and homozygous mouse tail genomic DNA, a 361-bp band was generated due to the single residual LoxP site and the short linker remaining in the $G\alpha_{i2}$ gene after Cre-recombinase action. The G184Sneo allele is not detected due to the large size of the PCR product. (D) Confirmation of the G184S mutation in mouse tail DNA. A PCR fragment amplified with primers (a and b) flanking the G184S mutation was subjected to PvuI digestion and sequencing to confirm the presence of the mutation. (E) Western blotting of $G\alpha_{i2}$ from protein extracts from heart, liver, and brain of a wild-type and a homozygous $G\alpha_{i2}^{G184S/G184S}$ mouse. The membrane was stripped and reblotted with a Gβ antibody as a loading control. This blot is representative of three different protein preparations.

total kinase are averages of three separate samples which were run and blotted under identical conditions.

Telemetric measurement of heart rate and activity. A biocompatible ETA-F20 radiotransmitter (Data Sciences International, St. Paul, MN) was implanted intraabdominally into male mice (about 20 g body weight) under isoflurane anesthesia. After surgery, mice were allowed to recover for 14 days. Physical activity index, electrocardiographic traces, and body temperature were recorded for 5 min every hour for 72 h via telemetry in individually housed, nonanesthetized, freely moving animals. Data were acquired and analyzed using Dataquest A.R.T. 3.1 software (Data Science International).

Echocardiography. Mice were sedated with 1.5% isoflurane and placed in a supine position. Two-dimensionally guided M-mode recordings were obtained by an experienced operator as previously described (4). Scans were from a short-axis view at the level of the papillary muscles with either an Acuson Sequoia system with an Acuson 15-MHz linear-array transducer or a GE Vivid 7 system with a GE S10-MHz phased-array transducer (General Electric).

Statistical analyses. Comparisons of individual group means used a two-tailed Student's *t* test. Two-way analysis of variance (ANOVA) with Bonferroni post-test was used to compare multiple data sets. All statistical calculations were done using GraphPad Prism version 4 (GraphPad Software Inc., San Diego, Calif.).

RESULTS AND DISCUSSION

$G\alpha_{i2}^{G184S}$ knock-in mice are viable but at low rates. To elucidate the in vivo role of RGS proteins in the function of $G\alpha_{i2}$, genomic knock-in mice carrying the RGS-insensitive mutant $G\alpha_{i2}^{G184S}$ allele were generated. The mutant mice show early lethality, as the genotypes do not appear in the expected Mendelian ratios (Table 1). Both homozygous and heterozygous $G\alpha_{i2}^{G184S}$ mice obtained from heterozygote crosses are underrepresented at weaning (3 weeks of age) (Table 1). There are only one-third as many homozygotes (G184S/G184S) as wild type (+/+), and even the heterozygotes (+/G184S) are found at a frequency lower than expected (1.33 times the +/+ frequency, rather than twice their number). The deviation from the expected ratio is highly significant (χ^2 of 47.5, df 2; $P < 0.0001$). The reduced proportion of +/G184S mice from +/G184S × +/G184S matings (1.33 times the number of +/+ littermates instead of 2 times; χ^2 of 13.6, df 1; $P < 0.0002$) probably involves both fetal and maternal contributions, as the +/+ × +/G184S matings show only a small and not statistically significant reduction in heterozygote offspring (0.86 of wt). Furthermore, there is some neonatal lethality, as we have seen evidence of fetal resorption (both resorbed fetuses were G184S/G184S genotype) and reduced numbers of homozygotes in embryonic day 13.5 MEFs (10:16:4 for +/+, +/G184S, and G184S/G184S). While the low number of homozygous embryos is not statistically significant due to the small *n*, the proportions (1.6× +/+ for +/G184S and 0.4× +/+ for G184S/G184S) are quite similar to those seen at weaning. The presence of a phenotype in heterozygotes as well as in homozygotes is expected given the gain-of-function nature of the G protein mutation. It is also consistent with our previously reported findings in cardiocytes differentiated from ES cells, where the $G\alpha_o^{+/G184S}$ heterozygotes showed strongly enhanced negative chronotropic responses to the A1 adenosine agonist PIA (25). The phenotype of mutant mice is not due to changes in the level of expression, since $G\alpha_{i2}$ protein amounts are comparable in heart, liver, and brain of wild-type and homozygous $G\alpha_{i2}^{G184S/G184S}$ mice (Fig. 1E).

Enhanced signaling through the Gi-coupled LPA receptor in $G\alpha_{i2}^{G184S}$ mouse embryonic fibroblasts. To assess the biochemical function of the mutant $G\alpha_{i2}$, MEFs derived from wild-type, heterozygous, and homozygous littermate embryos were prepared. LPA inhibits AC and acts as a strong mitogen towards fibroblasts and other cell types via pertussis toxin-sensitive processes (63). LPA-mediated inhibition of AC was measured in embryonic fibroblasts derived from both the homozygous and heterozygous mice (Fig. 2A). Forskolin-stimulated AC was unchanged (data not shown), but LPA-mediated inhibition was enhanced. Maximum inhibition of forskolin-stimulated AC by LPA was 37% for wild-type MEFs and 52% and 54% for $G\alpha_{i2}^{+/G184S}$ and $G\alpha_{i2}^{G184S/G184S}$, respectively ($n = 6$ to 9; $P < 0.05$, *t* test). In contrast to results for adenosine and carbachol signaling in ES-derived cardiocytes with this mutation (24), there was no significant shift in the 50% effective concentration for LPA-mediated AC inhibition (71, 95, and 80 nM for +/+, +/G184S, and G184S/G184S, respectively), and so the only change was in the maximum response.

TABLE 1. Genotype frequencies of $G\alpha_{i2}^{+/G184S} \times G\alpha_{i2}^{+/G184S}$ matings[a]

Genotype	$G\alpha_{i2}^{+/G184S} \times G\alpha_{i2}^{+/G184S}$		$G\alpha_{i2}^{+/G184S} \times$ C57BL/6J	
	n[b]	% with genotype[c] (ratio to +/+)	n[b]	% with genotype[c] (ratio to +/+)
+/+	145	37.5 (1.00)	37	53.9 (1.00)
+/G184S	193	49.9 (1.33)	33	46.1 (0.86)
G184S/G184S	49	12.7 (0.34)		

[a] The number (and ratio to +/+) of animals with the indicated genotype at weaning (3 weeks) is shown. $G\alpha_{i2}^{+/G184S}$ mice for the $G\alpha_{i2}^{+/G184S} \times G\alpha_{i2}^{+/G184S}$ cross are from the N4 generation against C57BL/6J. $G\alpha_{i2}^{+/G184S}$ mice from the $G\alpha_{i2}^{+/G184S} \times$ C57BL/6J cross are N5 against C57BL/6J.

[b] Number of animals in each genotype includes both males and females; there was no difference in sex ratio distribution.

[c] The observed proportions of the three genotypes from $G\alpha_{i2}^{+/G184S} \times G\alpha_{i2}^{+/G184S}$ matings are highly significantly different from the expected 1:2:1 proportions (χ^2, 47.5; $P < 0.0001$). The ratio of +/+ to heterozygotes (+/G184S) from the +/G184S × +/G184S crosses (1:1.33) is also significantly different (χ^2, 13.6; $P < 0.0002$). However, heterozygotes from the $G\alpha_{i2}^{+/G184S} \times$ C57BL/6J cross are slightly reduced but not significantly.

We also examined Akt and ERK activation in response to LPA. There is a modest LPA-mediated stimulation of Akt phosphorylation in wild-type MEFs, but this is markedly increased in both $G\alpha_{i2}^{+/G184S}$ and $G\alpha_{i2}^{G184S/G184S}$ MEFs (Fig. 2B and C). In contrast, ERK activation by LPA was only slightly enhanced by the $G\alpha_{i2}^{G184S}$ allele, if at all (Fig. 2D). Interestingly, previous studies failed to show LPA-induced activation of Akt in Rat-1 embryo fibroblasts (6) and showed only a modest enhancement in NIH 3T3 cells (23), and so the dramatic effect in our mutant cell lines is striking. For Akt, there was also a small increase in basal phosphorylation (when assessed as a ratio of P-Akt to Akt), but this was not statistically significant. It may be due to residual LPA present even at low (0.5%) serum concentrations. Importantly, the enhancement of Akt activation by LPA in the mutant cell lines was blocked by PTX pretreatment, while PTX did not significantly affect stimulation in the wt cells. Thus, Akt activation by LPA receptors and G_{i2} is strongly regulated by RGS proteins, and in the absence of RGS effects on $G\alpha_{i2}$ there is a shift from a non-PTX-sensitive process to a predominantly Gi-mediated Akt activation in the mutant cell lines.

The effects of $G\alpha_{i2}$ with the G184S mutation differ from those of the constitutively active GTPase-deficient $G\alpha_{i2}^{Q205L}$ allele in two respects. First, our $G\alpha_{i2}^{G184S}$ is still under control of receptors, and so it provides a hyperactive but more physiological stimulus pattern. Second, $\beta\gamma$ signaling is also enhanced with $G\alpha_{i2}^{G184S}$, since loss of RGS-mediated GAP activity leads to a prolonged Gα-GTP state with a concomitant increase in free or active $\beta\gamma$, while expression of the $G\alpha_{12}^{Q205L}$ mutant should not increase the amount of free $\beta\gamma$ but only produces stimuli mediated by the Gα subunit. Consistent with this, we found that receptor-dependent Gi regulation of both adenylyl cyclase and Akt in MEFs was significantly enhanced by either one or two copies of this $G\alpha_{i2}^{G184S}$ mutation, with the

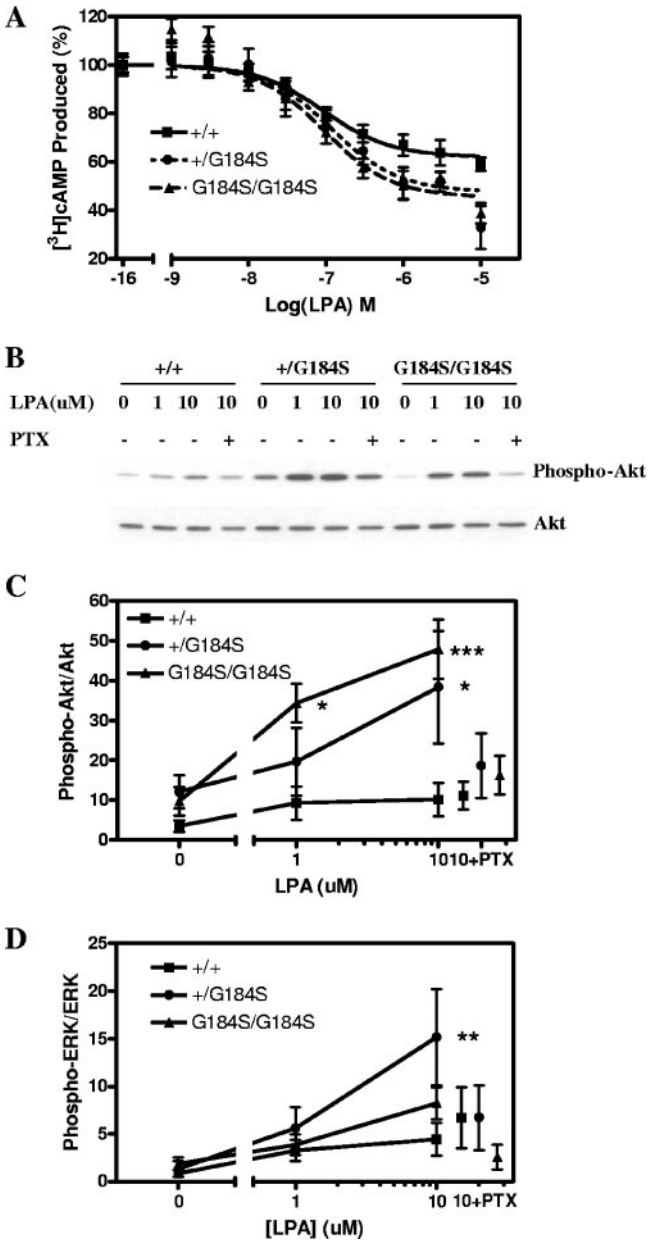

FIG. 2. Biochemical phenotype of $G\alpha_{i2}^{G184S}$ mouse embryonic fibroblast cells. (A) Lysophosphatidic acid inhibition of forskolin-stimulated AC. Dose-response curves for inhibition of AC by lysophosphatidic acid were determined from three individual embryonic fibroblast cell lines of each genotype. $n = 9$ for both +/+ and +/G184S, and $n = 6$ for G184S/G184S. Maximum inhibition among all three genotypes is different by F-test, $P < 0.005$. (B) PTX-sensitive phosphorylation/activation of Akt stimulated by LPA. MEF cells were stimulated with the indicated concentrations of LPA for 7.5 min. Cell lysates were analyzed by immunoblotting with an Akt phospho-specific antibody (Ser473). The membrane was stripped and reprobed with an antibody raised against total Akt. In some samples, the cells were incubated with PTX (100 ng/ml) overnight before stimulation with 10 μM LPA. (C and D) Western blotting and densitometric analysis of activation of Akt (C) and ERK (D) from averages of three independent experiments. The ratios of the densities of phosphorylated Akt or ERK to those for total Akt or ERK were calculated and are means ± standard errors of the means of three experiments. Significant differences from +/+ cells by two-way ANOVA with Bonferroni posttest are indicated as follows: *, $P < 0.05$; **, $P < 0.01$; ***, $P < 0.001$.

βγ-regulated phosphatidylinositol 3-kinase/Akt pathway being more strongly enhanced.

Growth retardation in $G\alpha_{i2}^{G184S}$ knock-in mice. The $G\alpha_{i2}^{G184S}$ knock-in mice showed a much more dramatic and complex phenotype affecting multiple organ systems (heart, myeloid, skeletal, and central nervous system) compared to the limited phenotype of $G\alpha_{i2}$-deficient mice (Table 2). The most apparent physiological phenotype of $G\alpha_{i2}^{G184S/G184S}$ mice is their small size (Fig. 3A). At 3 weeks of age, $G\alpha_{i2}^{G184S/G184S}$ mice had significantly reduced body weights (females [$P < 0.001$] and males [$P < 0.05$] by two-way ANOVA with Bonferroni posttest) compared to age- and sex-matched +/+ controls (Fig. 3B and C). The heterozygotes also showed significantly reduced body weights from 4 to 14 weeks for both males and females ($P < 0.001$ to 0.05). With aging, the body weight of $G\alpha_{i2}^{G184S/G184S}$ mice partially catches up with that of +/+ controls, but a significant difference still remains at 18 to 20 weeks ($P < 0.01$). Interestingly, mice deficient for $G\alpha_{i2}$ also displayed growth retardation that was apparent at 6 weeks of age (59), indicating that $G\alpha_{i2}$ plays an important role in both embryogenesis and neonatal growth, as described previously (47, 65). The pattern of low birth weight with significant "catch-up" for the $G\alpha_{i2}^{G184S/G184S}$ mice is different from dwarf mice with a growth hormone receptor knockout ($GHR^{-/-}$), where weights are nearly normal at birth but rapidly lose ground to their wild-type littermates (15). The pattern seen for the $G\alpha_{i2}^{G184S/G184S}$ mice is more reminiscent of the transgenic growth hormone antagonist-expressing mice (15). Reduced growth hormone could contribute to the small size, but the increased activity could also contribute (see below). There was

TABLE 2. Comparison of phenotypes of RGS-insensitive $G\alpha_{i2}^{G184S}$ mice and $G\alpha_{i2}$-deficient mice

Mouse type	Group	Phenotype
RGS-insensitive $G\alpha_{i2}^{G184S}$	General	Pre-/neonatal lethality (homozygote $G\alpha_{i2}^{G184S/G184S}$ and heterozygote $G\alpha_{i2}^{+/G184S}$)
		Low body weight
		Short bones
	Hematologic	Large spleen
		Increased monocyte and neutrophil counts
	Cardiac	Daytime tachycardia
		Increased heart organ weight/body weight ratio
		Hyperdynamic function
	Neurobehavioral	Hyperactivity
$G\alpha_{i2}$ deficient	General[a]	Pre- and postnatal lethality
		Growth retardation apparent at 6 wks of age
	Pathologic[a]	Ulcerative colitis and adenocarcinoma of colon
	Immunologic[a,b]	Increased no. of single positive (mature) T cells with high-intensity CD3 staining in thymus but unaffected lymphocyte homing in spleen
		Impaired marginal zone and B-1 B-cell development
	Hematologic[c]	Impaired platelet activation
	Cardiac[d]	Attenuated muscarinic inhibition of contractility and calcium currents in adult cardiomyocytes

[a] Based on references 58 and 59.
[b] Based on reference 16.
[c] Based on reference 35.
[d] Based on reference 52.

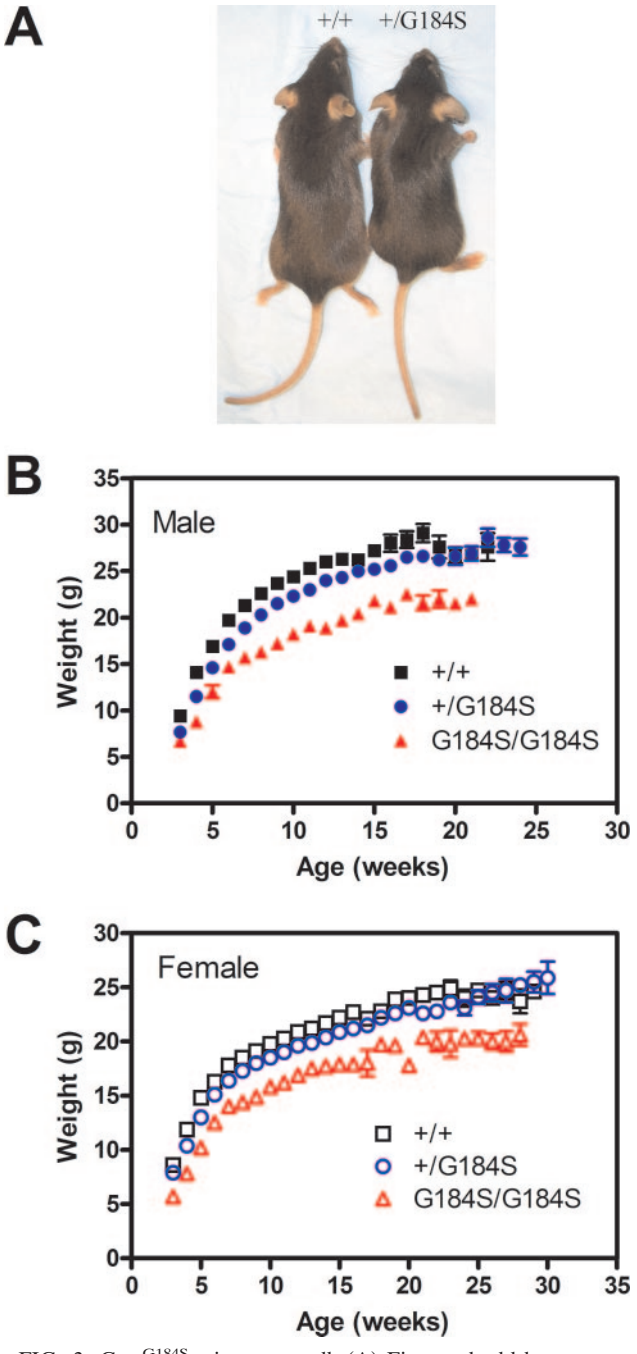

FIG. 3. $G\alpha_{i2}^{G184S}$ mice are small. (A) Five-week-old homozygous (right) and wt (left) male mice are shown. (B and C) wt (+/+), heterozygote (+/G184S), and homozygote (G184S/G184S) mice were weighed weekly, and means ± standard deviations are shown for male (B) and female (C) animals. Numbers of animals were as follows: +/+, 54 males, 57 females; +/G184S, 74 males, 78 females; G184S/G184S, 18 males, 21 females. Both homozygous and heterozygous mice had significantly reduced body weights compared to age- and sex-matched wt controls (see text for details).

not, however, any significant difference in either food intake or O_2 consumption (not shown).

Consistent with their decreased body weight, $G\alpha_{i2}^{G184S/G184S}$ mice also showed reduced body length (91.8 ± 1.1 [$n = 10$] versus 98.6 ± 0.7 for +/+ [$n = 9$]; $P < 0.001$, t test) and shorter bones (Fig. 4). They have a significant reduction in femur and tibia length compared with those of age- and sex-matched +/+ controls (Fig. 4). However, the size and morphology of the tibial growth plates were not significantly altered at 12 weeks of age (data not shown). One possible mechanism of the bone abnormalities could be a pseudohypoparathyroidism-like reduction in cAMP production. Patients with PHP-1a, which is caused by a heterozygous loss of function of $G\alpha_s$, have skeletal abnormalities, reduced responsiveness to parathyroid hormone, reduced serum calcium levels, and often mental retardation (1). A mouse model with a heterozygous mutant Gnas1 shows similar effects (70). Our $G\alpha_{i2}^{G184S/G184S}$ mice do not appear to be parathyroid hormone resistant, as they have normal serum calcium levels (not shown). Other features of PHP, such as obesity, subcutaneous ossifications, and brachydactyly, were also not observed.

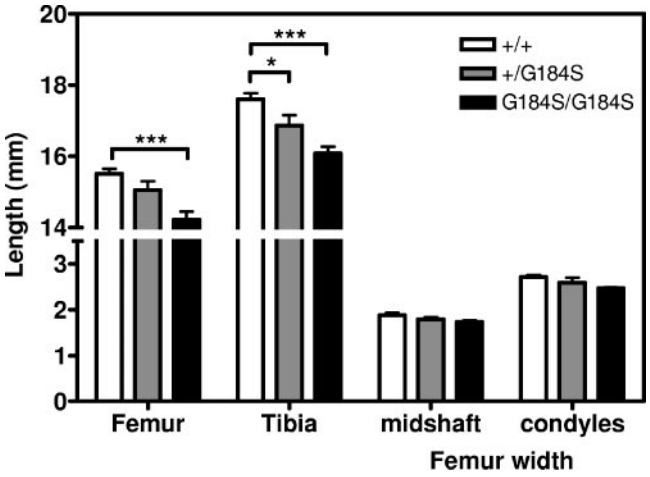

FIG. 4. $G\alpha_{i2}^{G184S}$ mice have skeletal abnormalities. Male mice of three genotypes (+/+, $n = 5$; +/G184S, $n = 2$; G184S/G184S, $n = 5$) were sacrificed, and bone length and width were measured using calipers. The genotype effect was highly significant by two-way ANOVA ($P < 0.0001$), and the tibia length was significantly shorter for mutant mice by a Bonferroni posttest (*, $P < 0.05$; ***, $P < 0.001$).

Hematologic abnormalities in $G\alpha_{i2}^{G184S}$ knock-in mice. Another striking observation was the marked splenomegaly in homozygous mutant mice ($P < 0.01$ by two-way ANOVA with Bonferroni posttest) (Fig. 5). The spleen/body weight ratio for female $G\alpha_{i2}^{G184S/G184S}$ mice (7.0 ± 0.80 mg/g) at 20 to 22 weeks of age was nearly double that of +/+ controls (3.7 ± 0.12 mg/g). A similar increase was also observed in males (not shown). In contrast, most other tissues (such as liver, kidney, lung, and uterus) retained their normal proportion to body weight. Peripheral blood counts showed no significant differences in total white blood cell, red blood cell, and platelet counts (Fig. 6A). However, homozygous $G\alpha_{i2}^{G184S/G184S}$ mice showed significantly elevated absolute neutrophil and monocyte counts (Fig. 6B) compared with wild-type mice. This result suggests an enhanced myeloid lineage differentiation, which would not be surprising given the role of $G\alpha_{i2}$ in neutrophil and monocyte function (3). Furthermore, transgenic expression of SDF-1/CXCL12 was recently shown to prevent myeloid precursor apoptosis in vitro and to increase myeloid differen-

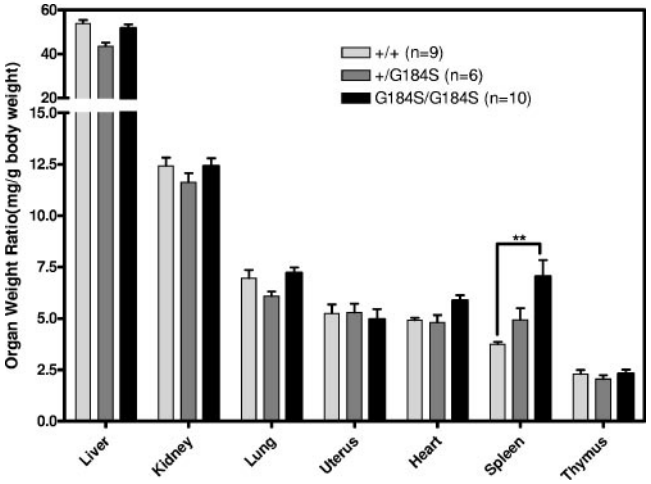

FIG. 5. Normalized organ weights as percentages of body weight. Female wild-type (+/+), heterozygote (+/G184S), and homozygote G184S/G184S mice were sacrificed between 20 and 22 weeks, organs were weighed, and weight ratios were calculated as mg organ weight/g body weight. **, $P < 0.01$ by two-way ANOVA with Bonferroni posttest.

tiation in vivo (5) by a mechanism involving CXCR4 and $G\alpha_i$. Since some endogenous SDF1a is found in myeloid precursor cells (27), the potentiated $G\alpha_{i2}$ signaling in our $G\alpha_{i2}^{G184S/G184S}$ mutant mice could have an effect similar to that which occurs with increased SDF-1/CXCL12 expression in the transgenic mice. Thus, increased survival and myelopoeisis may underlie the increased spleen size and peripheral neutrophil and monocyte counts seen in the mutant mice.

Homozygous $G\alpha_{i2}^{G184S}$ mice are hyperactive. Another significant effect is neurobehavioral. Based on data obtained during telemetry electrocardiographic monitoring, we observed that the $G\alpha_{i2}^{G184S/G184S}$ mice were more active during both day and night (Fig. 7). This is intriguing, since a knockout of RGS9 (which affects primarily $G\alpha_o$ and is localized to certain dopamine-related brain regions) shows an increased activity response to amphetamines and cocaine but no difference in unstimulated physical activity detected by beam-breaking in an activity chamber (56).

Cardiovascular alterations in $G\alpha_{i2}^{G184S}$ knock-in mice. In addition to the spleen, the heart was the one other organ that appeared to show an increase in mass relative to body weight in the mutants. This was true in females, with a 19% increase in heart weight/body weight ratio ($P < 0.01$ by t test) (Fig. 5), and was confirmed in males, with an 18% increase ($P < 0.02$ by t test) (Fig. 8B). In contrast to the spleen, there was not an increase in heart size in heterozygotes, though this could be due to the small magnitude of the effect of the mutation on heart size, even in homozygotes.

Along with the increased heart weight, the $G\alpha_{i2}^{G184S/G184S}$ homozygous mice showed an increase in baseline heart rate during the daytime (Fig. 8A). They also showed a hyperdynamic echocardiographic profile with a marked decrease in end systolic volume and a smaller but also statistically significant decrease in end diastolic volume (Fig. 8C). While fractional shortening and ejection fraction were slightly but not significantly increased, the end systolic volume even when corrected for body weight was dramatically reduced (0.23 versus 0.44 mm^3/g). The increased heart rate and evidence of increased contractility on echo suggest increased sympathetic tone. Indeed, the tachycardia in $G\alpha_{i2}^{G184S/G184S}$ mice was unexpected, since Gi mediates GIRK activation, which slows SA node rates. The in-

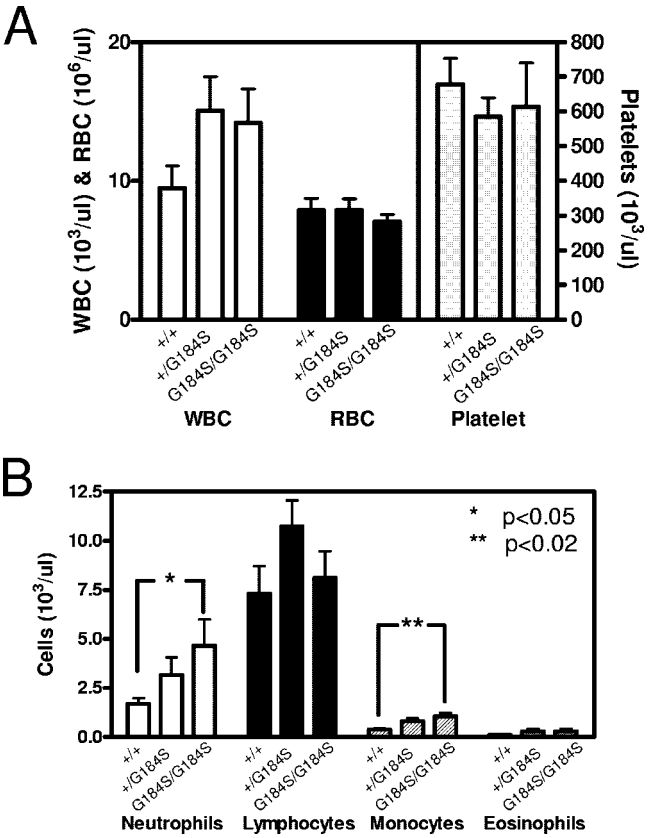

FIG. 6. $G\alpha_{i2}^{G184S/G184S}$ mice have elevated neutrophil and monocyte counts. Blood drawn from male and female mice (+/+, $n = 13$; +/G184S, $n = 4$; G184S/G184S, $n = 13$) via the lateral saphenous vein or from the orbital sinus of animals at sacrifice was collected in heparinized capillary tubes (Becton Dickson), and complete blood counts were done on a Coulter apparatus. Smears were stained, and differential counts were performed manually. Data are means ± standard errors of the means, and statistical significance of differences between +/+ and G184S/G184S was determined by t test (*, $P < 0.05$; **, $P < 0.02$).

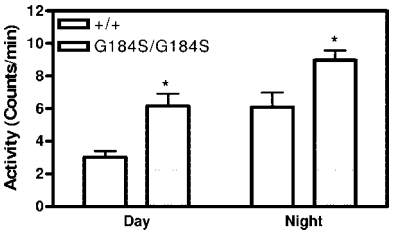

FIG. 7. Homozygous $G\alpha_{i2}^{G184S/G184S}$ mice are hyperactive. Activity data were captured for eight consecutive days with the activity detection feature of electrocardiography frequency transmitter (DSI) monitors on awake and unrestrained mice 16 weeks of age. Data are means ± standard errors of the means. Two-way ANOVA shows a significant effect of both genotype and time of day ($P < 0.0005$). *, $P < 0.05$ by Bonferroni posttest. $n = 5$.

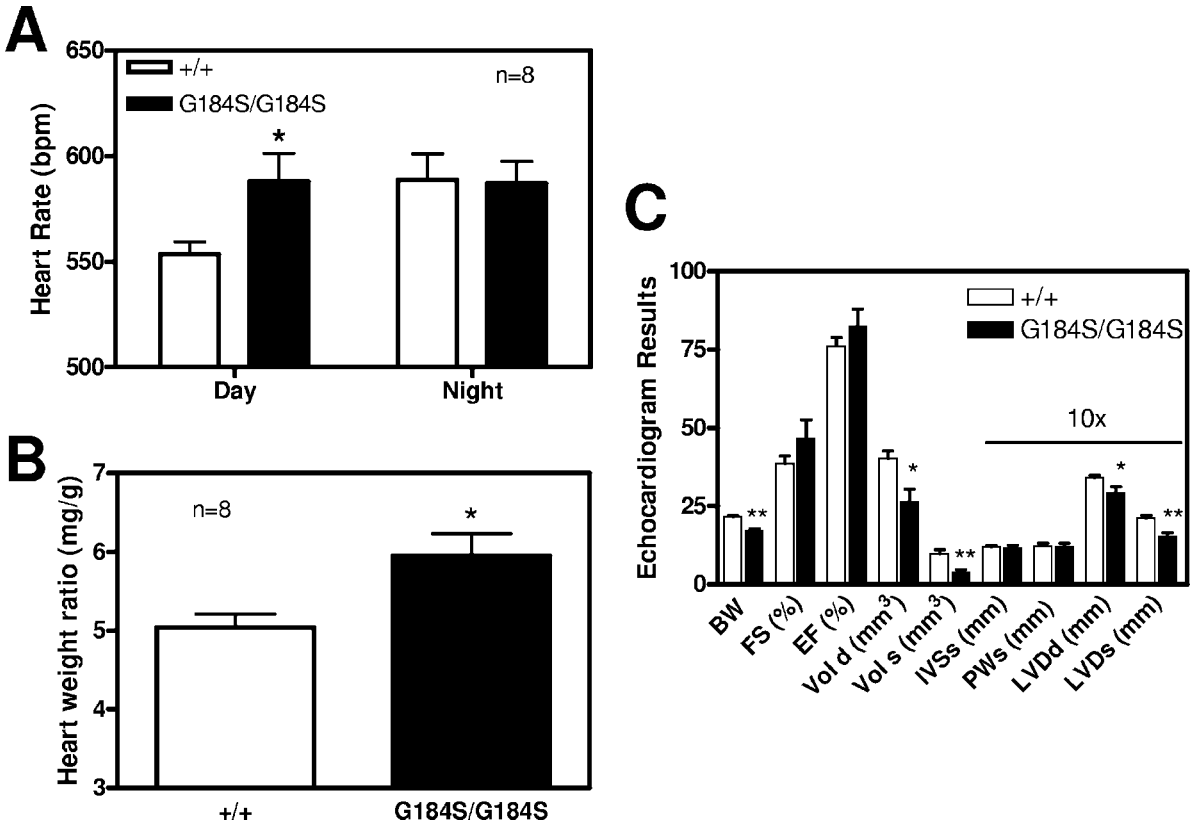

FIG. 8. Cardiovascular studies with homozygous $G\alpha_{i2}^{G184S/G184S}$ mice. (A) $G\alpha_{i2}^{G184S/G184S}$ mice have an increased daytime heart rate. Implanted electrocardiography frequency transmitters recorded the heart rate for 48 h, and the average heart rate was calculated for day and night from eight animals of each genotype. The G184S/G184S mutants showed increased daytime heart rate ($P < 0.05$). The larger error value for G184S/G184S in the daytime was due to one individual with a very high heart rate, but the difference was still significant ($P < 0.05$) with that value dropped. (B) $G\alpha_{i2}^{G184S/G184S}$ mice have enlarged hearts. Male mice (eight G184S/G184S and eight +/+ littermate controls) showed an increased heart weight/body weight ratio, confirming the observation in females (Fig. 5). The effect in males (20%) is of approximately the same magnitude as in females (19% increase; $P < 0.02$ by t test in Fig. 5). The difference between +/+ and G184S/G184S males is statistically significant ($P < 0.02$ by t test). (C) Echocardiographic measurements. Seven female +/+ and six female G184S/G184S mice at 13 to 15 weeks were studied under isoflurane anesthesia. Values of cardiac volume and left ventricular (LV) diameter, intraventricular septum and posterior wall were measured and fractional shortening and ejection fraction calculated. BW, body weight; FS, fractional shortening; EF, ejection fraction; Vol d, LV diastolic volume; Vol s, LV systolic volume; IVSs, intraventricular septum in systole; PWs, posterior wall in systole; LVDd, LV dimension in diastole; LVDs, LV dimension in systole. Values are means ± standard errors of the means, with statistical comparisons done by t test. *, $P < 0.05$; **, $P < 0.01$. $n = 7$.

creased heart rate was especially surprising in the face of our recent demonstration (24) that $G\alpha_{i2}^{G184S/G184S}$ mutant mice have dramatically enhanced muscarinic cholinergic bradycardia, which should lead to increased parasympathetic, rather than sympathetic, tone. Furthermore, cardiac overexpression of $G\alpha_s$ leads to tachycardia (67), while enhanced $G\alpha_i$ function should have the opposite effect. Thus, the increased heart rate is likely due to central nervous system effects—also reflected in the behavioral hyperactivity—rather than effects on cardiac function per se. Also, hyperactivation of Gi in heart by overexpression of a modified kappa opioid receptor (Ro1) leads to conduction defects and dilated cardiomyopathy, which appears to be opposite from our phenotype. Two differences in the models could account for this discrepancy (57). The overexpression of Ro1 could produce effects on its own, just as the tTA itself can lead to cardiomyopathy (45). Also, our enhanced Gi function may be more modest, given the need for a physiological stimulus to produce a response.

Given the increased heart size, we thus add $G\alpha_{i2}$ to the list of G proteins (including $G\alpha_s$ and $G\alpha_q$) whose enhanced signaling leads to cardiac hypertrophy. It could be related to either systemic alterations, such as increased sympathetic tone, or to enhanced intrinsic cardiac signaling through ERK (29, 61) or Akt (14) activation, which can both cause cardiac hypertrophy. If this were due to intrinsic cardiac signaling, it would probably be mediated by the $\beta\gamma$ subunit, which is the primary signaling molecule to ERK and Akt, since the $G\alpha_i$ subunit generally does not activate those pathways. We did find a significantly enhanced PTX-sensitive LPA-induced Akt activation in MEFs from these mice, consistent with this possibility.

Summary. The RGSi $G\alpha_{i2}^{G184S}$ mice described here demonstrate a major contribution of the RGS protein family to control of signaling by G_{i2} in multiple organ systems. Significant increases in AC inhibition and Akt activation were observed, while ERK signaling seemed less affected, at least in MEFs. Predicted results were seen, such as the recently reported enhancement of muscarinic bradycardia (24) and alter-

ations in myeloid activity, along with results contrary to expectations, such as tachycardia, behavioral hyperactivity, and cardiac hypertrophy. Also, unexpected effects on bone and general growth/metabolic function were revealed. Furthermore, $G\alpha_{i2}$ regulation by RGS proteins is important during development, as there is substantial neonatal lethality in the $G\alpha_{i2}^{G184S/G184S}$ mice and some even in heterozygotes. These mice and the general approach of using RGS-insensitive Gα subunits, besides demonstrating the role of RGS proteins, provide novel insights into subtype-selective signaling by Gi family G proteins, where other approaches such as expression of constitutively active Gα subunits will not reveal key functions mediated by βγ release. Furthermore, RGS-insensitive Gα subunits can help dissect the function of the similar and partially redundant $G\alpha_{i1}$, $G\alpha_{i2}$, and $G\alpha_{i3}$ proteins. We do not yet have a full picture of all of the physiological changes in these mice or a complete understanding of the precise mechanisms of all of the alterations, but the dramatic and pleiotropic phenotype reveals a substantial role for RGS proteins and $G\alpha_{i2}$ in a broad range of physiological functions.

ACKNOWLEDGMENTS

This work was supported by NIH grants R01-GM39561 (R.R.N.), Multidisciplinary Cardiovascular Research Training grant NIH T32 HL07853-06 at the University of Michigan (X.H.), and an American Heart Association Predoctoral Fellowship (Y.F.) and was also supported in part by the Michigan Diabetes, Research, and Training Center (NIH P60 DK20572), the University of Michigan Cancer Center (NIH P30 CA046592), the University of Rheumatic Diseases Center Core (NIH P30AR0483), the University of Michigan Gastrointestinal Hormone Research Core Center (NIH P30DK034933), and the Michigan Animal Models Consortium funded by the Michigan Economic Development Corporation and the Michigan Technology Tri-Corridor (grant 085P1000815).

We sincerely thank Susanne Mumby of the University of Texas Southwestern Medical Center for providing $G\alpha_{i2}$-specific antibody, Kimber Converso for performing the cardiac echo studies, and Min Liu for assistance in this project.

REFERENCES

1. **Bastepe, M., and H. Juppner.** 2005. GNAS locus and pseudohypoparathyroidism. Horm. Res. **63:**65–74.
2. **Berman, D. M., T. Kozasa, and A. G. Gilman.** 1996. The GTPase-activating protein RGS4 stabilizes the transition state for nucleotide hydrolysis. J. Biol. Chem. **271:**27209–27212.
3. **Bokoch, G. M., and A. G. Gilman.** 1984. Inhibition of receptor-mediated release of arachidonic acid by pertussis toxin. Cell **39:**301–308.
4. **Boluyt, M. O., K. Converso, H. S. Hwang, A. Mikkor, and M. W. Russell.** 2004. Echocardiographic assessment of age-associated changes in systolic and diastolic function of the female F344 rat heart. J. Appl. Physiol. **96:**822–828.
5. **Broxmeyer, H. E., S. Cooper, L. Kohli, G. Hangoc, Y. Lee, C. Mantel, D. W. Clapp, and C. H. Kim.** 2003. Transgenic expression of stromal cell-derived factor-1/CXC chemokine ligand 12 enhances myeloid progenitor cell survival/antiapoptosis in vitro in response to growth factor withdrawal and enhances myelopoiesis in vivo. J. Immunol. **170:**421–429.
6. **Burgering, B. M., and P. J. Coffer.** 1995. Protein kinase B (c-Akt) in phosphatidylinositol-3-OH kinase signal transduction. Nature **376:**599–602.
7. **Chen, C. K., M. E. Burns, W. He, T. G. Wensel, D. A. Baylor, and M. I. Simon.** 2000. Slowed recovery of rod photoresponse in mice lacking the GTPase accelerating protein RGS9-1. Nature **403:**557–560.
8. **Chen, H., and N. A. Lambert.** 2000. Endogenous regulators of G protein signaling proteins regulate presynaptic inhibition at rat hippocampal synapses. Proc. Natl. Acad. Sci. USA **97:**12810–12815.
9. **Cho, H., K. Harrison, and J. H. Kehrl.** 2004. Regulators of G protein signaling: potential drug targets for controlling cardiovascular and immune function. Curr. Drug Targets Immune Endocr. Metab. Disord. **4:**107–118.
10. **Chuang, H. H., M. Yu, Y. N. Jan, and L. Y. Jan.** 1998. Evidence that the nucleotide exchange and hydrolysis cycle of G proteins causes acute desensitization of G-protein gated inward rectifier K^+ channels. Proc. Natl. Acad. Sci. USA **95:**11727–11732.
11. **Clark, M. J., C. Harrison, H. Zhong, R. R. Neubig, and J. R. Traynor.** 2003. Endogenous RGS protein action modulates mu-opioid signaling through Gαo. Effects on adenylyl cyclase, extracellular signal-regulated kinases, and intracellular calcium pathways. J. Biol. Chem. **278:**9418–9425.
12. **Clark, M. J., R. R. Neubig, and J. R. Traynor.** 2004. Endogenous regulator of G protein signaling proteins suppress Gαo-dependent, mu-opioid agonist-mediated adenylyl cyclase supersensitization. J. Pharmacol. Exp. Ther. **310:**215–222.
13. **Clark, M. J., and J. R. Traynor.** 2005. Endogenous regulator of G protein signaling proteins reduce μ-opioid receptor desensitization and down-regulation and adenylyl cyclase tolerance in C6 cells. J. Pharmacol. Exp. Ther. **312:**809–815.
14. **Condorelli, G., A. Drusco, G. Stassi, A. Bellacosa, R. Roncarati, G. Iaccarino, M. A. Russo, Y. Gu, N. Dalton, C. Chung, M. V. Latronico, C. Napoli, J. Sadoshima, C. M. Croce, and J. Ross, Jr.** 2002. Akt induces enhanced myocardial contractility and cell size in vivo in transgenic mice. Proc. Natl. Acad. Sci. USA **99:**12333–12338.
15. **Coschigano, K. T., A. N. Holland, M. E. Riders, E. O. List, A. Flyvbjerg, and J. J. Kopchick.** 2003. Deletion, but not antagonism, of the mouse growth hormone receptor results in severely decreased body weights, insulin, and insulin-like growth factor I levels and increased life span. Endocrinology **144:**3799–3810.
16. **Dalwadi, H., B. Wei, M. Schrage, K. Spicher, T. T. Su, L. Birnbaumer, D. J. Rawlings, and J. Braun.** 2003. B cell developmental requirement for the G alpha i2 gene. J. Immunol. **170:**1707–1715.
17. **Dascal, N.** 2001. Ion-channel regulation by G proteins. Trends Endocrinol. Metab. **12:**391–398.
18. **Day, P. W., J. J. Tesmer, R. Sterne-Marr, L. C. Freeman, J. L. Benovic, and P. B. Wedegaertner.** 2004. Characterization of the GRK2 binding site of Gαq. J. Biol. Chem. **279:**53643–53652.
19. **DiBello, P. R., T. R. Garrison, D. M. Apanovitch, G. Hoffman, D. J. Shuey, K. Mason, M. I. Cockett, and H. G. Dohlman.** 1998. Selective uncoupling of RGS action by a single point mutation in the G protein alpha-subunit. J. Biol. Chem. **273:**5780–5784.
20. **Doggrell, S. A.** 2004. Is RGS-2 a new drug development target in cardiovascular disease? Expert Opin. Ther. Targets **8:**355–358.
21. **Doupnik, C. A., N. Davidson, H. A. Lester, and P. Kofuji.** 1997. RGS proteins reconstitute the rapid gating kinetics of Gβγ-activated inwardly rectifying K^+ channels. Proc. Natl. Acad. Sci. USA **94:**10461–10466.
22. **Druey, K. M., K. J. Blumer, V. H. Kang, and J. H. Kehrl.** 1996. Inhibition of G-protein-mediated MAP kinase activation by a new mammalian gene family. Nature **379:**742–746.
23. **Fang, X., S. Yu, R. LaPushin, Y. Lu, T. Furui, L. Z. Penn, D. Stokoe, J. R. Erickson, R. C. Bast, Jr., and G. B. Mills.** 2000. Lysophosphatidic acid prevents apoptosis in fibroblasts via G_i-protein-mediated activation of mitogen-activated protein kinase. Biochem. J. **352:**135–143.
24. **Fu, Y., X. Huang, H. Zhong, R. M. Mortensen, L. D'Alecy, and R. R. Neubig.** 2006. Endogenous RGS proteins and Gα subtypes differentially control muscarinic and adenosine-mediated chronotropic effects. Circ. Res. **67:**266–274.
25. **Fu, Y., H. Zhong, M. Nanamori, R. M. Mortensen, X. Huang, K. Lan, and R. R. Neubig.** 2004. RGS-insensitive G-protein mutations to study the role of endogenous RGS proteins. Methods Enzymol. **389:**229–243.
26. **Grillet, N., A. Pattyn, C. Contet, B. L. Kieffer, C. Goridis, and J. F. Brunet.** 2005. Generation and characterization of Rgs4 mutant mice. Mol. Cell. Biol. **25:**4221–4228.
27. **Guo, Y., G. Hangoc, H. Bian, L. M. Pelus, and H. E. Broxmeyer.** 2005. SDF-1/CXCL12 enhances survival and chemotaxis of murine embryonic stem cells and production of primitive and definitive hematopoietic progenitor cells. Stem Cells **23:**1324–1332.
28. **Han, S. B., C. Moratz, N. N. Huang, B. Kelsall, H. Cho, C. S. Shi, O. Schwartz, and J. H. Kehrl.** 2005. Rgs1 and Gnai2 regulate the entrance of B lymphocytes into lymph nodes and B cell motility within lymph node follicles. Immunity **22:**343–354.
29. **Harris, I. S., S. Zhang, I. Treskov, A. Kovacs, C. Weinheimer, and A. J. Muslin.** 2004. Raf-1 kinase is required for cardiac hypertrophy and cardiomyocyte survival in response to pressure overload. Circulation **110:**718–723.
30. **Hart, M. J., X. Jiang, T. Kozasa, W. Roscoe, W. D. Singer, A. G. Gilman, P. C. Sternweis, and G. Bollag.** 1998. Direct stimulation of the guanine nucleotide exchange activity of p115 RhoGEF by Gα13. Science **280:**2112–2114.
31. **Hepler, J. R.** 2003. RGS protein and G protein interactions: a little help from their friends. Mol. Pharmacol. **64:**547–549.
32. **Hepler, J. R., D. M. Berman, A. G. Gilman, and T. Kozasa.** 1997. RGS4 and GAIP are GTPase-activating proteins for Gqα and block activation of phospholipase Cβ by γ-thio-GTP-Gqα. Proc. Natl. Acad. Sci. USA **94:**428–432.
33. **Heximer, S. P., R. H. Knutsen, X. Sun, K. M. Kaltenbronn, M. H. Rhee, N. Peng, A. Oliveira-dos-Santos, J. M. Penninger, A. J. Muslin, T. H. Steinberg, J. M. Wyss, R. P. Mecham, and K. J. Blumer.** 2003. Hypertension and prolonged vasoconstrictor signaling in RGS2-deficient mice. J. Clin. Investig. **111:**1259.
34. **Hollinger, S., and J. R. Hepler.** 2002. Cellular regulation of RGS proteins:

modulators and integrators of G protein signaling. Pharmacol. Rev. **54:**527–559.
35. **Jantzen, H. M., D. S. Milstone, L. Gousset, P. B. Conley, and R. M. Mortensen.** 2001. Impaired activation of murine platelets lacking $G\alpha_{i2}$. J. Clin. Investig. **108:**477–483.
36. **Jeong, S. W., and S. R. Ikeda.** 2001. Differential regulation of G protein-gated inwardly rectifying K^+ channel kinetics by distinct domains of RGS8. J. Physiol. **535:**335–347.
37. **Jeong, S. W., and S. R. Ikeda.** 2000. Endogenous regulator of G-protein signaling proteins modify N-type calcium channel modulation in rat sympathetic neurons. J. Neurosci. **20:**4489–4496.
38. **Koch, W. J., H. A. Rockman, P. Samama, R. A. Hamilton, R. A. Bond, C. A. Milano, and R. J. Lefkowitz.** 1995. Cardiac function in mice overexpressing the beta-adrenergic receptor kinase or a beta ARK inhibitor. Science **268:** 1350–1353.
39. **Koelle, M. R., and H. R. Horvitz.** 1996. EGL-10 regulates G protein signaling in the C. elegans nervous system and shares a conserved domain with many mammalian proteins. Cell **84:**115–125.
40. **Kozasa, T., X. Jiang, M. J. Hart, P. M. Sternweis, W. D. Singer, A. G. Gilman, G. Bollag, and P. C. Sternweis.** 1998. p115 RhoGEF, a GTPase activating protein for Gα12 and Gα13. Science **280:**2109–2111.
41. **Lan, K. L., N. A. Sarvazyan, R. Taussig, R. G. Mackenzie, P. R. DiBello, H. G. Dohlman, and R. R. Neubig.** 1998. A point mutation in Gαo and Gαi1 blocks interaction with regulator of G protein signaling proteins. J. Biol. Chem. **273:**12794–12797.
42. **Lan, K. L., H. Zhong, M. Nanamori, and R. R. Neubig.** 2000. Rapid kinetics of regulator of G-protein signaling (RGS)-mediated Gαi and Gαo deactivation. Gα specificity of RGS4 AND RGS7. J. Biol. Chem. **275:**33497–33503.
43. **Lewandoski, M., K. M. Wassarman, and G. R. Martin.** 1997. Zp3-cre, a transgenic mouse line for the activation or inactivation of loxP-flanked target genes specifically in the female germ line. Curr. Biol. **7:**148–151.
44. **Lodowski, D. T., J. A. Pitcher, W. D. Capel, R. J. Lefkowitz, and J. J. Tesmer.** 2003. Keeping G proteins at bay: a complex between G protein-coupled receptor kinase 2 and Gβγ. Science **300:**1256–1262.
45. **McCloskey, D. T., L. Turnbull, P. M. Swigart, A. C. Zambon, S. Turcato, S. Joho, W. Grossman, B. R. Conklin, P. C. Simpson, and A. J. Baker.** 2005. Cardiac transgenesis with the tetracycline transactivator changes myocardial function and gene expression. Physiol. Genomics **22:**118–126.
46. **Moratz, C., K. Harrison, and J. H. Kehrl.** 2004. Regulation of chemokine-induced lymphocyte migration by RGS proteins. Methods Enzymol. **389:** 15–32.
47. **Moxham, C. M., Y. Hod, and C. C. Malbon.** 1993. Induction of G alpha i2-specific antisense RNA in vivo inhibits neonatal growth. Science **260:**991–995.
48. **Mukhopadhyay, S., and E. M. Ross.** 1999. Rapid GTP binding and hydrolysis by Gq promoted by receptor and GTPase-activating proteins. Proc. Natl. Acad. Sci. USA **96:**9539–9544.
49. **Mumby, S. M., and A. G. Gilman.** 1991. Synthetic peptide antisera with determined specificity for G protein alpha or beta subunits. Methods Enzymol. **195:**215–233.
50. **Mumby, S. M., R. A. Kahn, D. R. Manning, and A. G. Gilman.** 1986. Antisera of designed specificity for subunits of guanine nucleotide-binding regulatory proteins. Proc. Natl. Acad. Sci. USA **83:**265–269.
51. **Murga, C., L. Laguinge, R. Wetzker, A. Cuadrado, and J. S. Gutkind.** 1998. Activation of Akt/protein kinase B by G protein-coupled receptors. A role for alpha and beta gamma subunits of heterotrimeric G proteins acting through phosphatidylinositol-3-OH kinase γ. J. Biol. Chem. **273:**19080–19085.
52. **Nagata, K., C. Ye, M. Jain, D. S. Milstone, R. Liao, and R. M. Mortensen.** 2000. $G\alpha_{i2}$ but not $G\alpha_{i3}$ is required for muscarinic inhibition of contractility and calcium currents in adult cardiomyocytes. Circ. Res. **87:**903–909.
53. **Neubig, R. R., and D. P. Siderovski.** 2002. Regulators of G-protein signalling as new central nervous system drug targets. Nat. Rev. Drug Disc. **1:**187–197.
54. **Nishiguchi, K. M., M. A. Sandberg, A. C. Kooijman, K. A. Martemyanov, J. W. Pott, S. A. Hagstrom, V. Y. Arshavsky, E. L. Berson, and T. P. Dryja.** 2004. Defects in RGS9 or its anchor protein R9AP in patients with slow photoreceptor deactivation. Nature **427:**75–78.
55. **Pace, A. M., M. Faure, and H. R. Bourne.** 1995. Gi2-mediated activation of the MAP kinase cascade. Mol. Biol. Cell **6:**1685–1695.
56. **Rahman, Z., J. Schwarz, S. J. Gold, V. Zachariou, M. N. Wein, K. H. Choi, A. Kovoor, C. K. Chen, R. J. DiLeone, S. C. Schwarz, D. E. Selley, L. J. Sim-Selley, M. Barrot, R. R. Luedtke, D. Self, R. L. Neve, H. A. Lester, M. I. Simon, and E. J. Nestler.** 2003. RGS9 modulates dopamine signaling in the basal ganglia. Neuron **38:**941–952.
57. **Redfern, C. H., M. Y. Degtyarev, A. T. Kwa, N. Salomonis, N. Cotte, T. Nanevicz, N. Fidelman, K. Desai, K. Vranizan, E. K. Lee, P. Coward, N. Shah, J. A. Warrington, G. I. Fishman, D. Bernstein, A. J. Baker, and B. R. Conklin.** 2000. Conditional expression of a Gi-coupled receptor causes ventricular conduction delay and a lethal cardiomyopathy. Proc. Natl. Acad. Sci. USA **97:**4826–4831.
58. **Rudolph, U., M. J. Finegold, S. S. Rich, G. R. Harriman, Y. Srinivasan, P. Brabet, G. Boulay, A. Bradley, and L. Birnbaumer.** 1995. Ulcerative colitis and adenocarcinoma of the colon in G alpha i2-deficient mice. Nat. Genet. **10:**143–150.
59. **Rudolph, U., M. J. Finegold, S. S. Rich, G. R. Harriman, Y. Srinivasan, P. Brabet, A. Bradley, and L. Birnbaumer.** 1995. Gi2 alpha protein deficiency: a model of inflammatory bowel disease. J. Clin. Immunol. **15:**101S–105S.
60. **Salomon, Y., C. Londos, and M. Rodbell.** 1974. A highly sensitive adenylate cyclase assay. Anal. Biochem. **58:**541–548.
61. **Sanna, B., O. F. Bueno, Y. S. Dai, B. J. Wilkins, and J. D. Molkentin.** 2005. Direct and indirect interactions between calcineurin-NFAT and MEK1-extracellular signal-regulated kinase 1/2 signaling pathways regulate cardiac gene expression and cellular growth. Mol. Cell. Biol. **25:**865–878.
62. **Siderovski, D. P., B. Strockbine, and C. I. Behe.** 1999. Whither goest the RGS proteins? Crit. Rev. Biochem. Mol. Biol. **34:**215–251.
63. **Swarthout, J. T., and H. W. Walling.** 2000. Lysophosphatidic acid: receptors, signaling and survival. Cell Mol. Life Sci. **57:**1978–1985.
64. **Swiatek, P. J., and T. Gridley.** 1993. Perinatal lethality and defects in hindbrain development in mice homozygous for a targeted mutation of the zinc finger gene Krox20. Genes Dev. **7:**2071–2084.
65. **Takano, K., S. Asano, and N. Yamashita.** 1994. Activation of G protein-coupled K^+ channels by dopamine in human GH-producing cells. Am. J. Physiol. Endocrinol. Metab. **266:**E318–E325.
66. **Todaro, G. J., and H. Green.** 1963. Quantitative studies of the growth of mouse embryo cells in culture and their development into established lines. J. Cell Biol. **17:**299–313.
67. **Uechi, M., K. Asai, M. Osaka, A. Smith, N. Sato, T. E. Wagner, Y. Ishikawa, H. Hayakawa, D. E. Vatner, R. P. Shannon, C. J. Homcy, and S. F. Vatner.** 1998. Depressed heart rate variability and arterial baroreflex in conscious transgenic mice with overexpression of cardiac Gsα. Circ. Res. **82:**416–423.
68. **Wade, S. M., W. K. Lim, K. L. Lan, D. A. Chung, M. Nanamori, and R. R. Neubig.** 1999. G_i activator region of α_{2A}-adrenergic receptors: distinct basic residues mediate G_i versus G_s activation. Mol. Pharmacol. **56:**1005–1013.
69. **Watson, N., M. E. Linder, K. M. Druey, J. H. Kehrl, and K. J. Blumer.** 1996. RGS family members: GTPase-activating proteins for heterotrimeric G-protein alpha-subunits. Nature **383:**172–175.
70. **Yu, S., D. Yu, E. Lee, M. Eckhaus, R. Lee, Z. Corria, D. Accili, H. Westphal, and L. S. Weinstein.** 1998. Variable and tissue-specific hormone resistance in heterotrimeric Gs protein alpha-subunit (Gsα) knockout mice is due to tissue-specific imprinting of the Gsα gene. Proc. Natl. Acad. Sci. USA **95:** 8715–8720.
71. **Zachariou, V., D. Georgescu, N. Sanchez, Z. Rahman, R. DiLeone, O. Berton, R. L. Neve, L. J. Sim-Selley, D. E. Selley, S. J. Gold, and E. J. Nestler.** 2003. Essential role for RGS9 in opiate action. Proc. Natl. Acad. Sci. USA **100:**13656–13661.
72. **Zhong, H., and R. R. Neubig.** 2001. Regulator of G protein signaling proteins: novel multifunctional drug targets. J. Pharmacol. Exp. Ther. **297:**837–845.